Mechanistic insight into B(C₆F₅)₃ catalyzed imine reduction with PhSiH₃ under stoichiometric water conditions†

Yunqing He, [ID] ‡*[a] Wanli Nie, [ID] ‡*[b] Ying Xue [ID] [c] and Qishan Hu[d]

A DFT and experimental study on the mechanism of B(C₆F₅)₃ catalyzed imine reduction is performed using PhSiH₃ as reductant under stoichiometric water conditions. Ingleson's path B is reconfirmed here. And four novel (C₆F₅)₃B−OH₂ induced pathways (paths C2, C3, D2 and D3) entirely different from all the previous mechanisms were determined for the first time. They are all B(C₆F₅)₃ and water/amine catalyzed cycles, in which the nucleophilic water or amine catalyzed addition step between PhSiH₃ and the *N*-silicon amine cation is the rate-determining step of paths C2/D2 and C3/D3 with activation Gibbs free energy barriers of 23.9 and 18.3 kcal mol⁻¹ in chloroform, respectively, while the final desilylation of the *N*-silicon amine cation depends on an important intermediate, (C₆F₅)₃B−OH⁻. The competitive behavior of the 5 paths can explain the experimental facts perfectly; if all the reactants and catalysts are added into the system simultaneously, water amount and nucleophiles (excess water and produced/added amine) provide on−off selectivity of the pathways and products. 1 eq. water leads to quick formation of (C₆F₅)₃B−OH⁻, leading to B-II being turned off, and nucleophiles like excess water and produced/added amine switch on CD-II, leading to production of the amine. B-I′ of Ingleson's path B is the only mechanism for anhydrous systems, giving *N*-silicon amine production only; B-I and C-I are competitive paths for systems with no more than 1 eq. water, producing the *N*-silicon amine and the [PhHC=NHPh]⁺[(C₆F₅)₃B−OH]⁻ ion pair; and paths C2, C3, D2 and D3 are competitive for systems with 1 eq. water and nucleophiles like excess water or added/produced amine, directly giving amination products.

1 Introduction

Reductive amination of carbonyl compounds (Scheme 1, which includes two steps: the condensation step with water generation first, and then the imine reduction) represents an efficient one-step approach to a variety of amines and is of significant importance in the chemical, biochemical and polymer industries.[1] In recent years, frustrated Lewis pairs (FLPs), especially B(C₆F₅)₃-based ones, have been widely considered as prospective non-metallic catalysts capable of effectively activating H₂ or Si–H as hydride sources in the catalytic reduction of imines and enamines.[2,3] It is *a priori* assumed that any reaction system involving B(C₆F₅)₃ requires strictly anhydrous conditions,[4] so an imine (or enamine) must be synthesized and dehydrated in advance.

Recently, Ashley and Stephan's research groups reported the hydrogenation of aldehydes catalyzed by B(C₆F₅)₃ in reagent grade polar solvents under high pressure of H₂, in which the authors suggested that B(C₆F₅)₃ has sufficient water tolerance that a small amount of water in the solvent does not affect the activity of the catalyst in polar solvents; Soós and coworkers developed a boron/nitrogen-centered FLP with remarkably high water tolerance; and Chang and coworkers reported a one-pot borane catalyzed reductive amination/hydrosilylation of α,β-unsaturated aldehydes, producing β-silylated secondary amines.[5] In 2016, Ingleson's research team reported

ᵃFaculty of Materials and Chemical Engineering, Computational Physics Key Laboratory of Sichuan Province, Yibin University, Yibin, Sichuan 64400, China. E-mail: yunqing0228@163.com
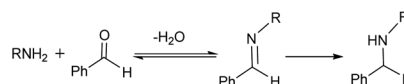
ᵇNatural Products and Small Molecule Catalysis Key Laboratory of Sichuan Province, Leshan Normal University, Leshan, Sichuan 614000, China. E-mail: niewl126@126.com

ᶜCollege of Chemistry, Sichuan University, Chengdu 610064, China

ᵈSchool of Chemistry and Chemical Engineering, Sichuan University of Arts and Science, Dazhou, Sichuan 635000, China
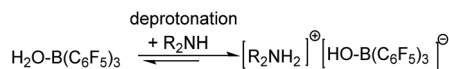
† Electronic supplementary information (ESI) available: (1) The Gibbs free energy changes of some binary and ternary adducts relative to the corresponding single molecules. (2) The Gibbs free energy profile of path A. (3) The optimized structures of the stationary points of the reactants and products, and the stationary points of B-I′/B-I and B-II in path B. (4) Optimized Cartesian coordinates of the stationary points. See DOI: 10.1039/d1ra02399c

‡ Yunqing He and Wanli Nie contributed equally to this article.

Scheme 1 Reductive amination.

Scheme 2 Deprotonation of $(C_6F_5)B-OH_2$ with amines.

Scheme 3 The mechanisms previously proposed for imine reduction by Ingleson *et al.* and Wei *et al.*

a successful one-pot reductive amination of aldehydes catalyzed by BAr$_3$ in the presence of hydridosilanes. Based on the viewpoint of dissociative borane catalysis, and its poor tolerance to water/amine combinations, Ingleson suggested that $B(C_6F_5)_3$ is only a viable catalyst for arylamines but not alkylamines due to the irreversible deprotonation of $(C_6F_5)_3B-OH_2$ by the latter (Scheme 2);[6] that is to say irreversible formation of $(C_6F_5)_3B-OH^-$ was disadvantageous to the reaction process. On the other hand, the acidity of $(C_6F_5)_3B-OH_2$ is comparable to that of hydrochloric acid.[7] Broadbelt *et al.* proposed a transition state in which $(C_6F_5)_3B-OH_2$ donates a proton in ring-opening reactions of epoxyoctane.[8] Our group recently confirmed that $B(C_6F_5)_3$ catalyzed reductive amination of aldehydes with alkoxyamines can proceed under moist conditions with hydridosilanes as reducing agents.[9]

The mechanistic study of FLP chemistry under "water or moist" conditions has attracted great attention. Imine reduction is a key process in reductive amination reactions, and the mechanism of borane catalyzed imine reduction under water conditions is a burning question. Ingleson *et al.* proposed two alternative catalytic cycles to explain the reduction of the imine intermediate in the borane catalyzed reductive amination.[6] Based on Ingleson's work, a density functional theory (DFT) study was performed by Wei *et al.* on the mechanism of $B(C_6F_5)_3$ catalyzed reductive amination under wet conditions, in which Ingleson's cycles were believed to be disfavored for high barriers and another path with very low barriers was suggested.[10] But we noted that a four-molecule elementary reaction step is involved in Wei's pathway which in fact makes it barely possible kinetically.[11] In all the paths proposed by Ingleson *et al.* and Wei *et al.*, imine cations PhHC=N$^+$RPh (R = H or {Si}) and $(C_6F_5)_3B-H^-$ are considered as key intermediates (Scheme 3), and amine should certainly be produced under water conditions. However, this is not consistent with our experiments; we have found that water amount and nucleophiles are very crucial for producing different hydrosilylation or amination products (see Table 1). The interaction between the Lewis base (LB), water and $B(C_6F_5)_3$ may play an important role in the reductive process, and perhaps some Si–H bond activation processes which do not produce $(C_6F_5)_3B-H^-$ should be considered.

In this work, we present a DFT computational and experimental investigation into the mechanism of $B(C_6F_5)_3$ catalyzed imine reduction with PhSiH$_3$ under water conditions, and eight reaction pathways are reported (see Scheme 4). Paths A and B are Ingleson's catalytic cycles which were determined to be disfavored for high barriers by Wei *et al.* using PhSiMe$_2$H; here we reconfirmed them using PhSiH$_3$. The $(C_6F_5)_3B-OH_2$ induced paths C1–C3 and D1–D3 are newly proposed and completely different from the above cycles, in that $(C_6F_5)_3B-OH^-$ is the key intermediate, and nucleophilic reagents like water or amines play an important role. As shown in Scheme 4, the imine cation

generation step(s) (C-I or D-I), addition step (CD-II) and desilylation step (CD-III) are involved in paths Cn and Dn; C-I involves a direct proton transfer from $(C_6F_5)_3B-OH_2$ to the imine, giving an imine cation, and direct proton transfer from $(C_6F_5)_3B-OH_2$ to the amine occurs first in D-I. The pathways involving C-I and D-I are denoted as paths Cn and Dn, respectively. And then the pathways involving CD-II without nucleophile assistance are denoted as paths C1/D1, and those that involve water assisted and amine assisted CD-II are denoted as paths C2/D2 and paths C3/D3, respectively.

2 Computational details

The computational study was performed using the Gaussian 16 program package.[12] All geometry optimizations and corresponding frequency analyses were performed at the B3LYP/6-311G(d,p) level in the gas phase, and the relationships between the transition states and the intermediates were verified with intrinsic reaction coordinate (IRC)[13] calculations. Solvent effect correction was done at the B3LYP/6-311G(d,p) level with Grimme's D3 BJ dispersion correction[14] using the SMD model[15–17] in chloroform. Single point energies in the solvent were combined with the thermodynamic corrections in the gas phase to obtain the Gibbs free energies in chloroform. Gibbs free energies are used in the following discussion and dissociated $B(C_6F_5)_3$ is selected as zero for comparison of different mechanisms. Transition states and intermediates are denoted as TS and IM in the following discussion, respectively. The optimized Cartesian coordinates of the stationary points are given in the ESI.†

3 Results and discussion

3.1 Experimental data

The influence of water and amine on $B(C_6F_5)_3$ catalyzed imine reduction using PhSiH$_3$ under water conditions is studied experimentally. As shown in Table 1, entries 1–4 give the corresponding hydrosilylation products in imine (PhCH=N–Ph/–*t*Bu) reduction systems containing 0 or 1 equiv. water with respect to the imine, while amination products were formed for entries 5 and 6 upon simply increasing the amount of water to 2 equiv. with respect to the imine, and entries 7 and 8 give the corresponding amination products, with just a slight difference (0.2 equiv. Et$_2$NH is used) compared to entries 3 and 4.

3.2 Computational data

3.2.1 The most stable initial complexes in anhydrous and water containing systems. There are complex interactions in reaction systems, and knowing the initial forms of the species is
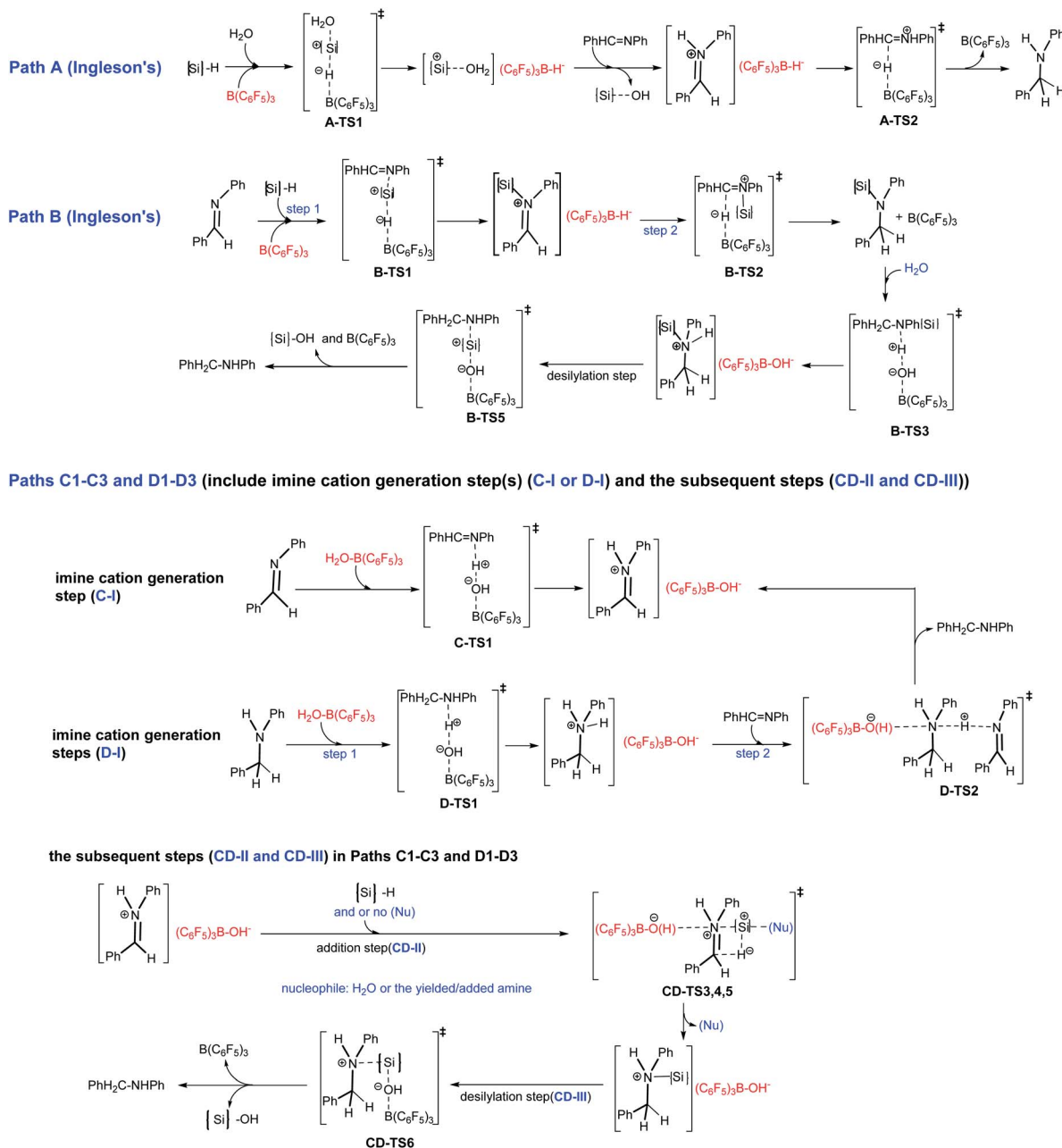
Scheme 4 Possible pathways of the title reaction.

crucial for understanding reaction selectivity and mechanisms. As shown in Table S1,† our DFT calculations demonstrate that the most stable initial complexes are the binary complex PhHC=PhN---B(C₆F₅)₃ (IM0) in anhydrous systems, and (C₆F₅)₃B---O(H)–H---NPh=CHPh (IM1) and (C₆F₅)₃B---O(H)–H---NH(Ph)–CH₂Ph (IM2) under water conditions, and the optimized structures of the complexes are shown in Fig. 1. So, IM0 is the starting point in anhydrous systems, and IM1 and IM2 are the starting points for paths Bn and Cn under water conditions.

3.2.2 Ingleson's catalytic cycles (paths A and B). The Gibbs free energy profile of path A in chloroform is shown in Fig. S1,† which demonstrates that path A is impossible under water

conditions due to the high Gibbs free energy barrier of A-TS1 (31.6 kcal mol⁻¹); this result is similar to that of Wei *et al.* for PhSiMe₂H.

Here we give an abbreviated presentation of path B for necessity of discussion. The energy profile of path B is shown in Fig. 2, and the optimized structures of the reactants and products, the stationary points in the *N*-silicon amine forming process (B-I′ and B-I in Fig. 2 for anhydrous and water containing conditions, respectively) and the stationary points in the subsequent steps (B-II) are shown in Fig. S2–S4,† respectively. Path B (IM1 → PhH₂C–NHPh) is a possible pathway under water conditions due to its low Gibbs free energy barriers (19.9, 4.3, 4.8 and 15.9 kcal mol⁻¹ for B-TS1, B-TS2, B-TS4 and B-TS5,

Table 1 Experimental data for imine reduction catalyzed by $B(C_6F_5)_3^a$

Entry	Imines	H_2O equiv.	Et_2NH equiv.	Temp. (°C)/time	Main products (% yield)
1	PhCH=N–Ph	0	0	30/12 h	$PhCH_2NPhSiH_2Ph$ (100)
2	PhCH=N–tBu	0	0	50/12 h	$PhCH_2NtBuSiH_2Ph$ (100)
3	PhCH=N–Ph	1	0	30/12 h	$PhCH_2NPhSiH_2Ph$ (100)
4	PhCH=N–tBu	1	0	50/12 h	$PhCH_2NtBuSiH_2Ph$ (100)
5	PhCH=N–Ph	2	0	30/12 h	$PhCH_2NHPh$ (100)
6	PhCH=N–tBu	2	0	50/12 h	$PhCH_2NHtBu$ (100)
7	PhCH=N–Ph	1	0.2	30/12 h	$PhCH_2NHPh$ (60)
8	PhCH=N–tBu	1	0.2	50/12 h	$PhCH_2NHtBu$ (83)

^{a} Reaction conditions: imine 0.1 mmol; hydrosilane 0.15 mmol; $B(C_6F_5)_3$ 10 mol%; solvent: $CDCl_3$; products were determined by ^1H NMR spectroscopy.

respectively, and no barrier for B-TS3). B-TS4 is a transition state for N–Si rotation. While IM0 → N-silicon amine (B-I′) may be the mechanism of imine reduction in anhydrous conditions, without subsequent hydrolysis and desilylation.

3.2.3 Paths C1–C3 and D1–D3

3.2.3.1 Imine cation generation steps (C-I and D-I)

3.2.3.1.1 Imine cation generation step C-I. As shown in Fig. 3, IM1 is turned into the imine cation $PhHC=N^+HPh$ and $(C_6F_5)_3B–OH^-$ anion *via* C-TS1 with a Gibbs free energy barrier of 1.8 kcal mol^{-1}. The only imaginary frequency of C-TS1 is 355.82i cm^{-1} and its vibrational mode corresponds to the transfer of H2 from O1 to N1; the B–O1, O1–H2 and N1–H2 interatomic distances in C-TS1 are 1.58, 1.13 and 1.40 Å, respectively. In CD-IM3, the B–O1, O1–H2 and N1–H2 interatomic distances are 1.52, 1.60 and 1.07 Å, respectively, showing that the imine cation $PhHC=N^+HPh$ and $(C_6F_5)_3B–OH^-$ have been generated. Water acts as a protonic acid in this step.

3.2.3.1.2 Imine cation generation steps D-I. As shown in Fig. 3, IM2 is turned into the amine cation $PhH_2C–N^+H_2Ph$ and $(C_6F_5)_3B–OH^-$ anion *via* D-TS1 with no barrier. The only imaginary frequency of D-TS1 is 583.10i cm^{-1} and its vibrational mode corresponds to the transfer of H2 from O1 to N1′; the B–

O1, O1–H2 and N1′–H2 interatomic distances in D-TS1 are 1.54, 1.21 and 1.27 Å, respectively. In D-IM4, the B–O1, O1–H2 and N1′–H2 interatomic distances are 1.52, 1.43 and 1.12 Å, respectively, implying that the amine cation $PhH_2C–N^+H_2Ph$ and $(C_6F_5)_3B–OH^-$ have been produced. And then the amine cation gives a proton to N1 in the imine by D-TS2 with a Gibbs free energy barrier of 6.0 kcal mol^{-1} to produce the imine cation $PhHC=N^+HPh$ with the amine $PhH_2C–NHPh$ being regenerated simultaneously. The only imaginary frequency of D-TS2 is 836.56i cm^{-1} and its vibrational mode corresponds to the transfer of H3 from N1′ in the amine cation to N1 in the imine; the N1′–H3 and N1–H3 interatomic distances in D-TS2 are 1.44 and 1.21 Å, respectively. CD-IM3 is obtained after releasing the amine $PhH_2C–NHPh$.

3.2.3.2 The subsequent addition steps giving the N-silicon amine cation (CD-II)

3.2.3.2.1 Direct addition step. As shown in Fig. 4, H1$^-$ transfers from $PhSiH_3$ to C1 in $PhHC=N^+HPh$, and the Si of PhH_2Si^+ approaches N1 by CD-TS3 with a Gibbs free energy barrier of 41.4 kcal mol^{-1}, giving the N-silicon amine cation $PhH_2C–N^+HPh(SiH_2Ph)$. The only imaginary frequency of CD-TS3 is 415.94i cm^{-1} and its vibrational mode corresponds to
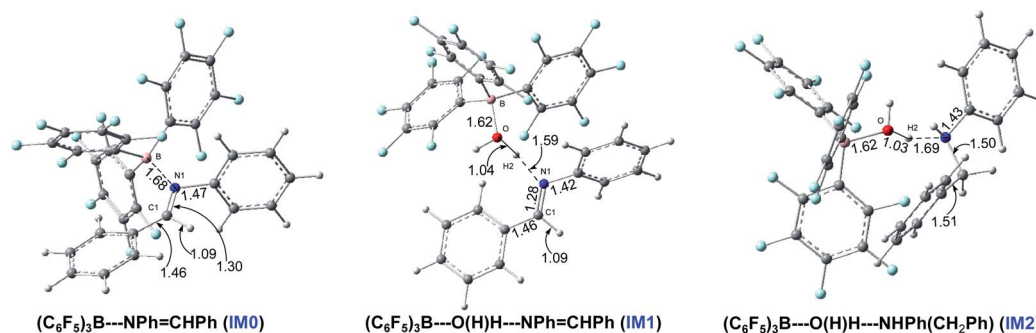

Fig. 1 The optimized structures of the initial complexes at the B3LYP/6-311G(d,p) level in the gas phase with corresponding interatomic distances in angstroms.
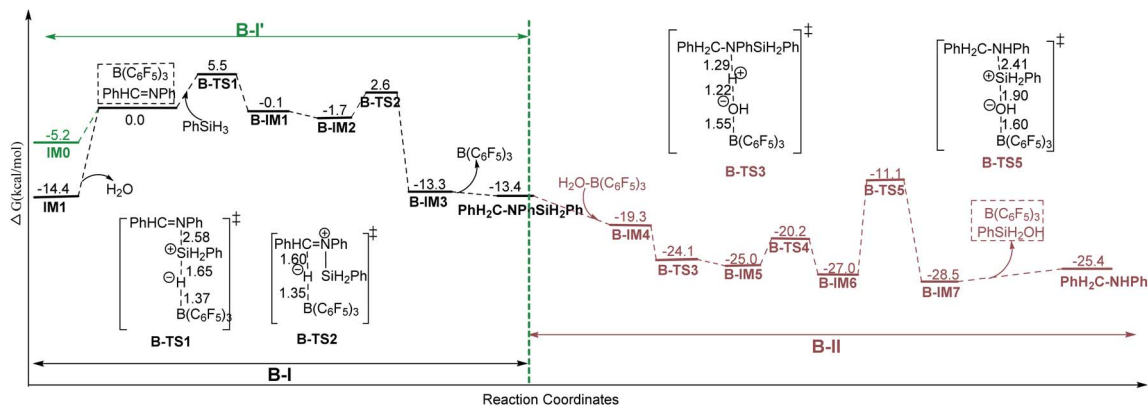
Fig. 2 The Gibbs free energy profile of path B in chloroform with corresponding distances in angstroms (unit: kcal mol^{-1}).

the transfer of H1 from Si to C1 and Si approaching N1; the C1–H1, Si–H1, N1–Si and C1–N1 interatomic distances in CD-TS3 are 1.20, 1.82, 2.53 and 1.43 Å, respectively. In CD-IM4, the C1–H1, N1–Si and C1–N1 distances are 1.09, 1.90 and 1.53 Å, respectively, implying that C1–H1 and N1–Si bonds have formed and C1=N1 has turned into a C1–N1 single bond. CD-IM5 is the most stable complex of the *N*-silicon amine cation and $(C_6F_5)_3B$–OH$^-$.

3.2.3.2.2 Water assisted addition step. As shown in Fig. 4, with the assistance of nucleophilic H_2O, H1$^-$ transfers from PhSiH$_3$ to C1 in PhHC=N$^+$HPh by CD-TS4 with a Gibbs free energy barrier of 23.9 kcal mol^{-1}. The only imaginary frequency of CD-TS4 is 377.91i cm^{-1} and its vibrational mode corresponds to the transfer of H1 from Si to C1 and O2 of H_2O approaching Si; the C1–H1, Si–H1, O2–Si and C1–N1 interatomic distances in CD-TS4 are 1.42, 1.67, 2.25 and 1.35 Å, respectively. When H1$^-$ is transferred to C1, PhH$_2$Si$^+$ is simultaneously attracted by O2 and the neighboring N1 with lone pair electrons. In CD-IM6, the C1–H1, O2–Si and N1–Si interatomic distances are 1.09, 2.56 and 1.96 Å, respectively, suggesting that the attraction from N1

is stronger than that from O2, an N1–Si bond is formed and the *N*-silicon amine cation PhH$_2$C–N$^+$HPh(SiH$_2$Ph) is produced; there is no bond formed between O2 and Si. CD-IM5 is obtained when CD-IM6 releases H_2O. Water acts as a catalyst to decrease the barrier of this step (23.9 kcal mol^{-1} for CD-TS4 *vs.* 41.4 kcal mol^{-1} for CD-TS3); the weak nucleophilicity of H_2O decreases the barrier of H1$^-$ transfer from Si to C1, and the $(C_6F_5)_3B$–OH$^-$ location and the O1---H2---N1 hydrogen bond increase the attraction of N1 to PhH$_2$Si$^+$.

3.2.3.2.3 Amine assisted addition step. When amine is produced in the system, it may assist the addition step just like water. As shown in Fig. 4, with the assistance of the amine PhH$_2$C–NHPh, H1$^-$ transfers from PhSiH$_3$ to C1 in PhHC=N$^+$HPh by CD-TS5 with a Gibbs free energy barrier of 18.3 kcal mol^{-1}. The only imaginary frequency of CD-TS5 is 425.87i cm^{-1} and its vibrational mode corresponds to the transfer of H1 from Si to C1 and N1′ of the amine approaching Si; the C1–H1, Si–H1, N1′–Si and C1–N1 interatomic distances in CD-TS5 are 1.50, 1.65, 2.44 and 1.34 Å, respectively. Similar to the water assisted addition step, PhH$_2$Si$^+$ is attracted by N1′ and
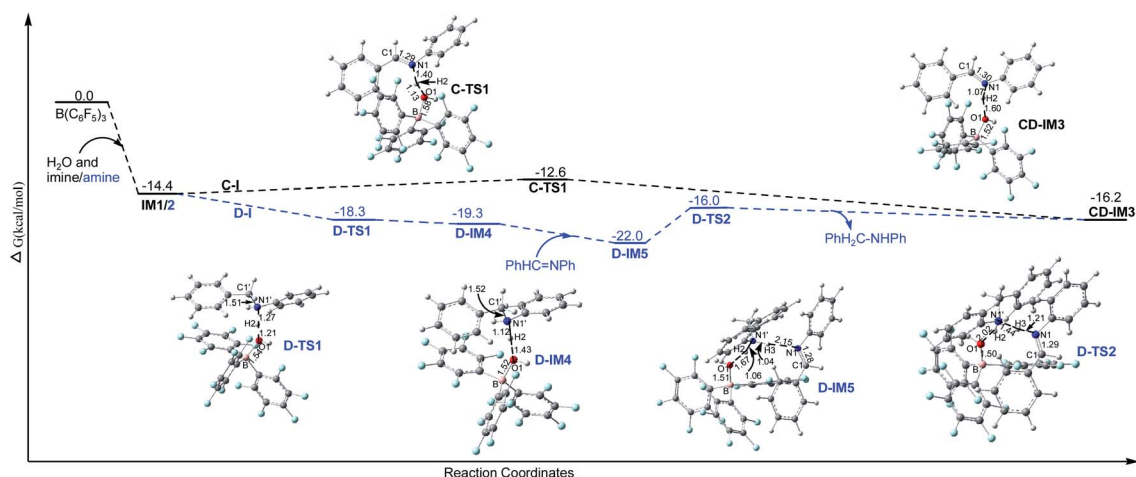

Fig. 3 The Gibbs free energy profiles of the imine cation generation steps C-I and D-I in chloroform with the corresponding interatomic distances in the optimized structures in angstroms (unit: kcal mol^{-1}, IM1 and IM2 share the same ΔG).
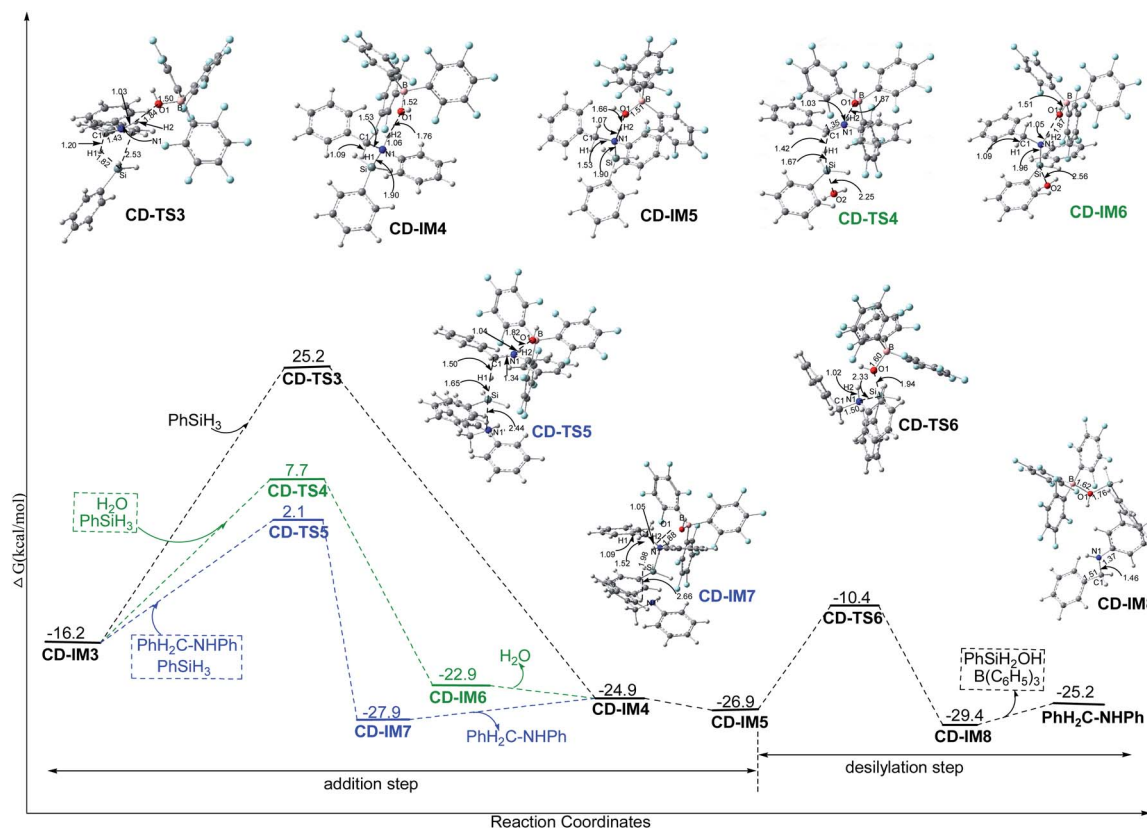
Fig. 4 The Gibbs free energy profiles of the addition and desilylation steps (CD-II and CD-III) in chloroform with the corresponding interatomic distances in the optimized structures in angstroms (unit: kcal mol^{-1}).

N1 simultaneously. In CD-IM7, the C1–H1, N1–Si and N1′–Si distances are 1.09, 1.98 and 2.66 Å, respectively, and an *N*-silicon amine cation is produced with N1–Si bond formation. The amine (PhH$_2$C–NHPh) acts as a catalyst to decrease the barrier of this step (18.3 kcal mol^{-1} for CD-TS5 *vs.* 41.4 kcal mol^{-1} for CD-TS3) even more; the nucleophilicity of the amine decreases the barrier of H1$^-$ transfer from Si to C1 tremendously, while the (C$_6$F$_5$)$_3$B–OH$^-$ location and the O1---H2---N1 hydrogen bond increase the attraction of N1 to PhH$_2$Si$^+$. CD-IM5 is obtained when CD-IM7 releases PhH$_2$C–NHPh.

3.2.3.3 The common final desilylation step. As shown in Fig. 4, the final step is that (C$_6$F$_5$)$_3$B–OH$^-$ attacks Si in the *N*-silicon amine cation by CD-TS6 with a Gibbs free energy barrier of 16.5 (for paths Cn) or 17.5 (for paths Dn) kcal mol^{-1}, producing PhSiH$_2$OH and amine PhH$_2$C–NHPh with B(C$_6$F$_5$)$_3$ regeneration. The only imaginary frequency of CD-TS6 is 130.10i cm^{-1} and its vibrational mode corresponds to the breaking of the N1–Si and B–O1 bonds and the formation of the Si–O1 bond. The N1–Si, Si–O1 and B–O1 interatomic distances in CD-TS6 are 2.33, 1.94 and 1.60 Å, respectively. CD-TS6 is similar to B-TS5 with the only difference being the orientation of the substituent groups on N1.

3.2.4 The competitive behavior of the five paths B, C2, C3, D2 and D3. The total steps and corresponding Gibbs free energy barriers of paths A, B, C1–C3 and D1–D3 are listed in Table 2.

Table 2 The total steps and corresponding Gibbs free energy barriers in paths A, B, C1–C3 and D1–D3 (unit: kcal mol^{-1})

Path A	Imine protonation and (C$_6$F$_5$)$_3$B–H$^-$ formation A-TS1/31.6		H$^-$ transfer to imine cation, giving amine A-TS2/4.6	
Path B	B-I: *N*-silicon amine generation steps B-TS1/19.9 B-TS2/4.3		B-II: hydrolysis for desilylation steps B-TS3/— B-TS4/1.8 B-TS5/15.9	

Paths Cn/Dn	Imine cation generation step(s)		CD-II: addition step	CD-III: common desilylation step
C1			CD-TS3/41.4	CD-TS6/16.5 for paths Cn; 17.5 for paths Dn
C2	C–I: C-TS1/1.8		CD-TS4/23.9	
C3			CD-TS5/18.3	
D1			CD-TS3/41.4	
D2	D-I: D-TS1/— D-TS2/6.0		CD-TS4/23.9	
D3			CD-TS5/18.3	

Paths Cn/Dn	Imine cation generation step(s)	CD-II: addition step	CD-III: common desilylation step
C1	C–I: C-TS1/1.8	CD-TS3/41.4	CD-TS6/16.5 for paths Cn;
C2		CD-TS4/23.9	17.5 for paths Dn
C3		CD-TS5/18.3	
D1	D-I: D-TS1/; D-TS2/ 6.0	CD-TS3/41.4	
D2		CD-TS4/23.9	
D3		CD-TS5/18.3	

Obviously, paths A, C1 and D1 are impossible due to their high barriers (31.6 and 41.4 kcal mol^{-1} for A-TS1 and CD-TS3, respectively). So, there are seemingly five competitive pathways (paths B, C2, C3, D2 and D3) for imine reduction under water conditions with PhSiH$_3$. Their competitive behavior (a graphical representation is shown in Fig. 5) is different in different systems, because (i) B-II needs the participation of dissociated B(C$_6$F$_5$)$_3$ and water, (ii) C-I and D-I consume B(C$_6$F$_5$)$_3$ and water which leads to quick formation of (C$_6$F$_5$)$_3$B–OH$^-$, (iii) whereas C-II and D-II need nucleophiles like excess water and produced/added amine as catalysts.

3.2.4.1 For stepwise imine reduction. Ingleson's path B is the only mechanism. The *N*-silicon amine is formed in anhydrous systems first along B-I′ (IM0 → *N*-silicon amine, see Fig. 2), and then water is added into the system to produce the amine along B-II. So only hydrosilylation products can be obtained in anhydrous conditions; this is consistent with entries 1 and 2 in Table 1.

3.2.4.2 For the one-time feeding method. For the one-time feeding method, all the reactants and catalysts were added into the system simultaneously. As illustrated in Fig. 2–5 and Table 2, water and nucleophiles (excess water and produced/added amine) provide on–off selectivity of the pathways and products.

(1) When the water amount is no more than 1 eq. without amine in the system, if only the barriers of their rate-determining steps are considered, one can say that paths B and C2 can proceed competitively, leading to amination products; this is inconsistent with entries 3 and 4 in Table 1. The competitive behavior of paths B and C2 is discussed as follows: The initial dominant presence of IM1 is favorable for C-I instead of B-I; the much lower barrier of C-TS1 (1.8 kcal mol^{-1}) than B-TS1 (19.9 kcal mol^{-1}) gives C-I a competitive advantage over B-I, so C-I dominates dynamically in comparison with B-I, suggesting that B(C$_6$F$_5$)$_3$ is turned into (C$_6$F$_5$)$_3$B–OH$^-$ quickly. This means that hydrolysis for desilylation (B-II) of the *N*-silicon amine can't proceed due to the lack of dissociated B(C$_6$F$_5$)$_3$ (*i.e.* B-II is turned off by C-I), and there is no remaining free water for the water assisted addition step (CD-IM3 → CD-TS4, CD-II) of path C2. Hence, in fact, just B-I and C-I proceed competitively, delivering the *N*-silicon amine and the [PhHC=NHPh]$^+$[(C$_6$F$_5$)$_3$B–OH]$^-$ ion pair, which is consistent with entries 3 and 4 in Table 1.

(2) When the water amount is more than 1 eq. without amine in the system, B-II still can't proceed due to the lack of free B(C$_6$F$_5$)$_3$, while the remaining free water after C-I means that the subsequent water assisted addition step (CD-IM3 → CD-TS4) in path C2 can proceed, and amine is finally yielded by the desilylation step; the yielded amine makes paths C3, D2, and D3 join the competition. These four pathways lead to amination products which is consistent with entries 5 and 6 in Table 1. Similarly, when 1 eq. water combined with a catalytic amount of amine is added into the system, amine will be produced by paths C3, C2, D3 and D2 competitively; this is consistent with entries 7 and 8 in Table 1. Obviously, nucleophilic excess water and produced/added amine open up the CD-II process and finally lead to amine production. Accordingly, the imine intermediate in reductive amination with PhSiH$_3$ should be reduced to amine through paths C3, C2, D3 and D2.

(3) Paths C2, C3, D2 and D3 can proceed successfully only when the water amount is above a critical amount (more than 1 eq. water is suggested for it is a key reactant in C-I and D-I). In brief, 1 eq. water leads to quick formation of (C$_6$F$_5$)$_3$B–OH$^-$, leading to B-II being turned off, and then nucleophiles like excess water and produced/added amine switch on CD-II, leading to the production of amine.

(4) When using the alkylamine Me$_2$NH instead of the produced arylamine, the Gibbs free energy of the ion pair [Me$_2$NH$_2$]$^+$(C$_6$F$_5$)$_3$B–OH$^-$ is located at -24.4 kcal mol^{-1} (lower than -19.3 kcal mol^{-1} for D-IM4, Fig. 3); this is disfavorable for producing the amine with high selectivity, and the arylamine is suggested to catalyze the addition step, which is consistent with entries 7 and 8 in Table 1 and Ingleson's result.

4 Conclusions

In systems of imine reduction with PhSiH$_3$ under stoichiometric water conditions, the most stable initial complex of B(C$_6$F$_5$)$_3$ is the ternary complex (C$_6$F$_5$)$_3$B---OH(H)---LB (LB is PhN=CHPh or PhH$_2$C–NHPh), which is convenient for the (C$_6$F$_5$)$_3$B–OH$_2$ induced reaction. Ingleson's path B is reconfirmed as one possible competitive pathway. And four novel B(C$_6$F$_5$)$_3$ and water/amine catalyzed competitive pathways (paths C2, C3, D2 and D3) induced by (C$_6$F$_5$)$_3$B–OH$_2$ were determined for the first time, in which the nucleophilic water or amine catalyzed addition step between PhSiH$_3$ and the *N*-silicon amine cation is the rate-determining step of paths C2/D2 and C3/D3 with Gibbs free energy barriers of 23.9 and 18.3 kcal mol^{-1} in chloroform, respectively, while (C$_6$F$_5$)$_3$B–OH$^-$ is an important intermediate and the final desilylation of the *N*-silicon amine cation depends on it. Water acts as a reactant in the imine cation generation step(s); water/amine (providing an appropriate nucleophilic electric field) acts as a catalyst in the addition step CD-II. The competitive behavior of paths B, C2, C3, D2 and D3 can explain the experimental facts perfectly. For the one-time feeding method of imine reduction under stoichiometric water conditions with PhSiH$_3$, water amount and nucleophiles (excess water and produced/added amine) provide on–off selectivity of the pathways and products. 1 eq. water leads to quick formation of (C$_6$F$_5$)$_3$B–OH$^-$, leading to the B-II
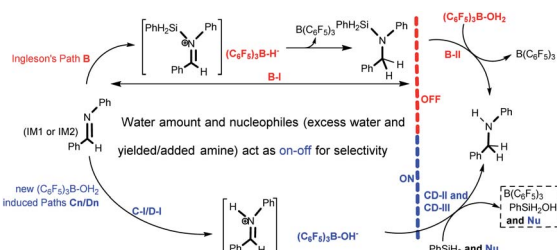

Fig. 5 The competitive behavior of paths B, C2, C3, D2 and D3 results in water and nucleophiles (excess water and produced/added amine) providing on–off selectivity for imine reduction with PhSiH$_3$ under water conditions.

path being closed, and nucleophiles like excess water and produced/added amine open up CD-II, leading to production of amine: (1) when the water amount is no more than 1 eq., the *N*-silicon amine and the ion pair $[\text{PhHC}{=}\text{NHPh}]^+[(C_6F_5)_3B{-}OH]^-$ are produced through competitive B-I and C-I; (2) when 1 eq. water is combined with a catalytic amount of arylamine or if more than 1 eq. water is added initially, amine will be produced by the competitive paths C2, C3, D2 and D3. In brief, B-I′ of Ingleson's path B is the only mechanism for anhydrous systems, giving *N*-silicon amine production only, B-I and C-I are competitive paths for systems with no more than 1 eq. water, producing the *N*-silicon amine and the ion pair $[\text{PhHC}{=}\text{NHPh}]^+[(C_6F_5)_3B{-}OH]^-$, and paths C2, C3, D2 and D3 are competitive for systems with 1 eq. water and nucleophiles like excess water or added/produced amine, directly giving amination products.

Conflicts of interest

The authors declare no conflict of interest.

Acknowledgements

References

1 (*a*) S. A. Lawrence, *Amines: Synthesis, Properties and Applications*, Cambridge University Press, Cambridge, U.K., 2005, Vol. 9, pp. 1015–1025; (*b*) T. C. Nugent and M. El-Shazly, *Adv. Synth. Catal.*, 2010, **352**, 753–819; (*c*) J. P. Wolfe, S. Wagaw, J. F. Marcoux and S. Buchwald, *Acc. Chem. Res.*, 1998, **31**, 805–818; (*d*) J. Zheng, T. Roisnel, C. Darcel and J.-B. Sortais, *ChemCatChem*, 2013, **5**, 2861–2864.

2 (*a*) D. J. Parks and W. E. Piers, *J. Am. Chem. Soc.*, 1996, **118**, 9440–9441; (*b*) J. M. Blackwell, K. L. Foster, V. H. Beck and W. E. Piers, *J. Org. Chem.*, 1999, **64**, 4887–4892; (*c*) G. C. Welch, R. R. San Juan, J. D. Masuda and D. W. Stephan, *Science*, 2006, **314**, 1124–1126; (*d*) G. C. Welch and D. W. Stephan, *J. Am. Chem. Soc.*, 2007, **129**, 1880–1881; (*e*) P. Spies, G. Erker, G. Kehr, K. Bergander, R. Fraeohlich, S. Grimme and D. W. Stephan, *Chem. Commun.*, 2007, 5072–5074; (*f*) D. W. Stephan and G. Erker, *Angew. Chem., Int. Ed.*, 2010, **49**, 46–76; (*g*) S. Tussing, L. Greb, S. Tamke, B. Schirmer, C. Muhle-Goll, B. Luy and J. Paradies, *Chem.–Eur. J.*, 2015, **21**, 8056–8059; (*h*) S. Tussing, K. Kaupmees and J. Paradies, *Chem.–Eur. J.*, 2016, **22**, 7422–7426.

3 (*a*) S. Rendler and M. Oestreich, *Angew. Chem., Int. Ed.*, 2008, **47**, 5997–6000; (*b*) J. Hermeke, M. Mewald and M. Oestreich, *J. Am. Chem. Soc.*, 2013, **135**, 17537–17546; (*c*) A. Y. Houghton, J. Hurmalainen, A. Mansikkamäki, W. E. Piers and H. M. Tuononen, *Nat. Chem.*, 2014, **6**, 983–988; (*d*) W. E. Piers, A. J. V. Marwitz and L. G. Mercier, *Inorg. Chem.*, 2011, **50**, 12252–12262; (*e*) J. Zhang, S. Park and S. Chang, *J. Am. Chem. Soc.*, 2018, **140**, 13209–13213; (*f*) J. Zhang and S. Chang, *J. Am. Chem. Soc.*, 2020, **142**, 12585–12590.

4 (*a*) J. M. Blackwell, E. R. Sonmor, T. Scoccitti and W. E. Piers, *Org. Lett.*, 2000, **2**, 3921–3923; (*b*) P. A. Chase, T. Jurca and D. W. Stephan, *Chem. Commun.*, 2008, 1701–1703; (*c*) Y.-B. Liu and H.-F. Du, *Acta Chim. Sin.*, 2014, **72**, 771–777.

5 (*a*) D. J. Scott, M. J. Fuchter and A. E. Ashley, *J. Am. Chem. Soc.*, 2014, **136**, 15813–15816; (*b*) D. J. Scott, T. R. Simmons, E. J. Lawrence, G. G. Wildgoose, M. J. Fuchter and A. E. Ashley, *ACS Catal.*, 2015, **5**, 5540–5544; (*c*) T. Mahdi and D. W. Stephan, *J. Am. Chem. Soc.*, 2014, **136**, 15809–15812; (*d*) T. Mahdi and D. W. Stephan, *Angew. Chem., Int. Ed.*, 2015, **54**, 8511–8514; (*e*) Á. Gyömöre, M. Bakos, T. Földes, I. Pápai, A. Domján and T. Soós, *ACS Catal.*, 2015, **5**, 5366–5372; (*f*) E. Dorkó, M. Szabó, B. Kótai, I. Pápai, A. Domján and T. Soós, *Angew. Chem., Int. Ed.*, 2017, **56**, 9512–9516; (*g*) E. Kim, S. Park and S. Chang, *Chem.–Eur. J.*, 2018, **24**, 5765–5769.

6 (*a*) V. Fasano, J. E. Radcliffe and M. J. Ingleson, *ACS Catal.*, 2016, **6**, 1793–1798; (*b*) V. Fasano and M. J. Ingleson, *Chem.–Eur. J.*, 2017, **23**, 2217–2224.

7 C. Bergquist, B. M. Bridgewater, C. J. Harlan, J. R. Norton, R. A. Friesner and G. Parkin, *J. Am. Chem. Soc.*, 2000, **122**, 10581–10590.

8 Y. Yu, Y. Zhu, M. N. Bhagat, A. Raghuraman, K. F. Hirsekorn, J. M. Notestein, S. T. Nguyen and L. J. Broadbelt, *ACS Catal.*, 2018, **8**, 11119–11133.

9 (*a*) C. Tian, Y. Jiang, M. Borzov and W.-L. Nie, *Acta Chim. Sin.*, 2015, **73**, 1203–1206; (*b*) X. Hu, C. Tian, Y. Jiang, M. Borzov and W.-L. Nie, *Acta Chim. Sin.*, 2015, **73**, 1025–1030; (*c*) Z.-G. Wen, C. Tian, Y. Jiang, M. Borzov and W.-L. Nie, *Acta Chim. Sin.*, 2016, **74**, 498–502; (*d*) W.-L. Nie, G.-F. Sun, C. Tian and M. Borzov, *Z. Naturforsch., B: J. Chem. Sci.*, 2016, **71**(10), 1029; (*e*) L.-W. Zhang, Z.-G. Wen, M. Borzov and W.-L. Nie, *Acta Chim. Sin.*, 2017, **75**, 819–823; (*f*) G.-F. Sun, M. Su, J. Fang, M. Borzov and W.-L. Nie, *Acta Chim. Sin.*, 2017, **75**, 824–830; (*g*) Y.-Q. He, J.-W. Teng, C. Tian, M. Borzov, Q.-Sh. Hu and W.-L. Nie, *Acta Chim. Sin.*, 2018, **76**, 774–778; (*h*) G.-F. Sun, Y.-Q. He, C. Tian, M. Borzov, Q.-S. Hu and W.-L. Nie, *Acta Chim. Sin.*, 2019, **77**, 166–171.

10 H.-C. Chen, L.-N. Yan and H.-Y. Wei, *Organometallics*, 2018, **37**, 3698–3707.

11 X. Fu, W. Shen, T. Yao, W. Hou, *Physical Chemistry*, Higher Education Press, Beijing, 2006, Vol. 2, pp. 154–213.

12 M. J. Frisch, G. W. Trucks, H. B. Schlegel, G. E. Scuseria, M. A. Robb, J. R. Cheeseman, G. Scalmani, V. Barone, G. A. Petersson, H. Nakatsuji, X. Li, M. Caricato, A. V. Marenich, J. Bloino, B. G. Janesko, R. Gomperts, B. Mennucci, H. P. Hratchian, J. V. Ortiz, A. F. Izmaylov, J. L. Sonnenberg, D. Williams-Young, F. Ding, F. Lipparini,

F. Egidi, J. Goings, B. Peng, A. Petrone, T. Henderson, D. Ranasinghe, V. G. Zakrzewski, J. Gao, N. Rega, G. Zheng, W. Liang, M. Hada, M. Ehara, K. Toyota, R. Fukuda, J. Hasegawa, M. Ishida, T. Nakajima, Y. Honda, O. Kitao, H. Nakai, T. Vreven, K. Throssell, J. A. Montgomery, J. E. Peralta Jr, F. Ogliaro, M. J. Bearpark, J. J. Heyd, E. N. Brothers, K. N. Kudin, V. N. Staroverov, T. A. Keith, R. Kobayashi, J. Normand, K. Raghavachari, A. P. Rendell, J. C. Burant, S. S. Iyengar, J. Tomasi, M. Cossi, J. M. Millam, M. Klene, C. Adamo, R. Cammi, J. W. Ochterski, R. L. Martin, K. Morokuma, O. Farkas, J. B. Foresman, and D. J. Fox, *Gaussian 16, Revision A.03*, Gaussian, Inc., Wallingford CT, 2016.

13 (*a*) C. Gonzalez and H. B. Schlegel, *J. Chem. Phys.*, 1989, **90**, 2154–2161; (*b*) C. Gonzalez and H. B. Schlegel, *J. Phys. Chem.*, 1990, **94**, 5523–5527; (*c*) W. J. Hehre, R. Ditchfield and J. A. Pople, *J. Chem. Phys.*, 1972, **56**, 2257–2261.

14 S. Grimme, S. Ehrlich and L. Goerigk, *J. Comput. Chem.*, 2011, **32**, 1456–1465.

15 S. Miertus and J. Tomasi, *Chem. Phys.*, 1982, **65**, 239–245.

16 M. Cossi, V. Barone, R. Cammi and J. Tomasi, *Chem. Phys. Lett.*, 1996, **255**, 327–335.

17 A. V. Marenich, C. J. Cramer and D. G. Truhlar, *J. Phys. Chem. B*, 2009, **113**, 6378–6396.